POAC'17
Busan, KOREA

Proceedings of the 24th International Conference on
Port and Ocean Engineering under Arctic Conditions
June 11-16, 2017, Busan, Korea

Local Ice Load on Ship Hulls
- An Approach from Model Testing -

Koh Izumiyama[1]
[1] Hokkaido University (Sapporo, Japan)

ABSTRACT

This paper discusses local ice load measurement in model testing. Studying local ice load is important in terms of both safety and performance of ships in ice. A tactile sensor system is used in model tests to measure local ice loads on the model. Model test results at NMRI ice tank are presented. The test was performed to study local ice loading from a viewpoint of ship safety in ice. A model ship with podded propulsors and a model ship with a conventional rudder and propeller system were tested in a free-running mode. Discussion is made of the calibration of the tactile sensor, ice load distributions, and comparison of the test results with full-scale data.

KEY WORDS: Local Ice Load; Tactile Sensor; Ice Tank Test

INTRODUCTION

Ships sailing in ice-covered waters are exerted by loads from the ice. Ice load is characterized as localized high load in comparison with hydrodynamic loads. Such local ice load is the foremost concern for the safety of ships in ice. Ship hull structures should be designed and constructed to withstand local ice loads to safeguard the people and cargoes on-board. Local ice load is also significant from the viewpoint of ship performance in ice. Ship resistance in ice can be given as a vector sum of local ice loads on the hull. Knowing the behavior of local ice load will deepen the understanding of ice resistance. In this way, local ice load is important in terms of both safety and performance of ships in ice.

Model testing in ice tanks provides useful data for ship-in-ice research. It is an indispensable tool for designing ice-going ships today. There have been some model studies done with local ice load measurements (e.g.: Liukkonen and Nortala-Hoikkanen, 1992; and Kayo, 1993). In these studies segmented models were tested. However, a segmented model with many load cells installed is a complicated model to manufacture. It is difficult to have many small segments in the model. This limits the spatial resolution of the local ice load measurement.

Recently, a tactile sensor system has been used for ice tank tests to measure local ice loads on the model. National Maritime Research Institute (NMRI) of Japan pioneered the use of tactile sensor for model testing in ice. A wide range of tests have been made at NMRI ice tank with tactile measurements. This includes an indentation test of a flat indentor (Izumiyama et al., 1999a), resistance test of a ship (Izumiyama et al., 1999b and Izumiyama et al., 2001), free-running test of ships (Matsuzawa et al., 2006 and Izumiyama et al., 2007) measurement of ice load on a conical structure and towing test of a drill ship in broken ice (Izumiyama et al., 2016). Model tests with the tactile sensor have also been performed at ice tanks of Aalto University (Valkonen et al., 2007 and Kujala and Arughadhoss, 2012) and Korea Research Institute of Ships and Ocean Engineering (Jeong et al., 2015).

This paper discusses the model test measurement of local ice load by way of the tactile sensor. From the above-mentioned model tests performed at NMRI ice tank, free-running test of ship models is presented. This test was made to study local ice load from a viewpoint of ship safety in ice. There have been full-scale measurements made on this issue for various ships and sea areas (e.g.: Hanninen, 2007). However, full-scale measurements are usually made in relatively small areas in the hull. It is difficult to see a whole picture of local ice loading over a ship hull. The model test was performed to have such a picture. In the following, the sensor system is briefly described first. This is followed by the presentation of the method and results of the model test. Finally discussion is made of the calibration of the tactile sensor, ice load distributions along the hull, and comparison of test results with full-scale data.

TACTILE SENSOR

Sensor Description

A tactile sensor system I-Scan is used for the model tests at NMRI ice tank. The system is composed of sensor films and software to acquire and process the data by a PC. Sensor films are connected to PC via handles. The sensor film is thin and flexible. This allows the film to be installed on the model hull surface by adhesive tapes without creating roughness that can affect model-ice interaction. The software displays in real time the measured pressure data. It also has functions to store the data as files and to export them as ASCII text files.

In a sensor film there are in total 1936 pressure sensing cells locating in a square latticed pattern of 44 rows by 44 columns. The manufacturer provides sensor films of different sizes. Sensor films with a sensing area of 238 mm square (I-Scan 210) are used for the ship model tests at NMRI ice tank. In this sensor film, sensing cells are located at 5.4 mm intervals at the center. Each sensing cell is of 3.5 mm square area and there are non-sensing gaps of about 2 mm between cells.

The output from the I-Scan system is not pressure but a digital counter called a “Raw” from 0 (no pressure) to 255 (maximum pressure). A “Row Sum” is a sum of Raws from sensing cells in the whole or a part of a sensor film. Calibration needs to be made for converting Raw into a pressure or force value. The method to calibrate the I-Scan system for the purpose of ice model tests will be discussed later in this paper.

Basic Characteristics of the Tactile Sensor

Prior to the use of I-Scan sensor system for the model testing in the ice tank, a series of trial tests were performed to obtain basic characteristics of the sensor. In the test, a sensor film with a 112 mm square sensing area (I-Scan 100) was loaded in three different ways of 1) stepwise loading, 2) sinusoidal loading and 3) creep test. Loads were applied in a 70 mm square area in the center of the sensor film via a rubber sheet. Raw Sum from the loaded area was analyzed. Test results are shown in Figure 1. Loads applied and I-Scan responses are summarized below.

- Stepwise Loading Test: The sensor film is loaded stepwise loads up to 10 kN. The response of I-Scan is somewhat non-linear in the high load region. There is slight hysteresis seen between the loading and unloading phases.
- Sinusoidal Loading Test: The sensor film is loaded by loads fluctuating between 2 kN and 8 kN in a sinusoidal pattern. Tests were made at different loading frequencies in a range from 0.1 Hz to 35 Hz. I-Scan shows a flat response to the loads through the frequency range of up to 35 Hz.
- Creep Test: The sensor film is loaded by static loads of 5 kN and 10 kN for a duration of about 300 seconds. Output Raw Sum shows some drift with time. Drifting rate is approximately 5%/min.

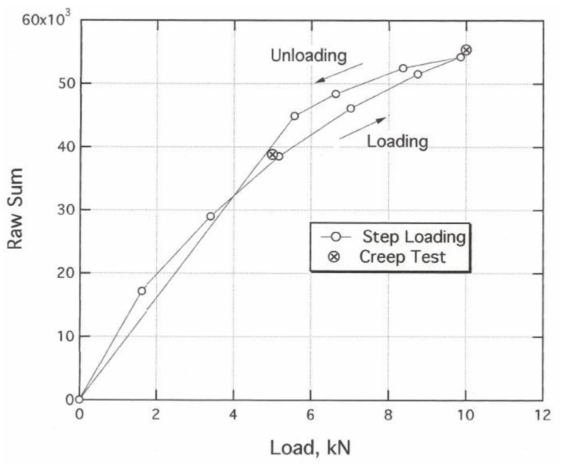

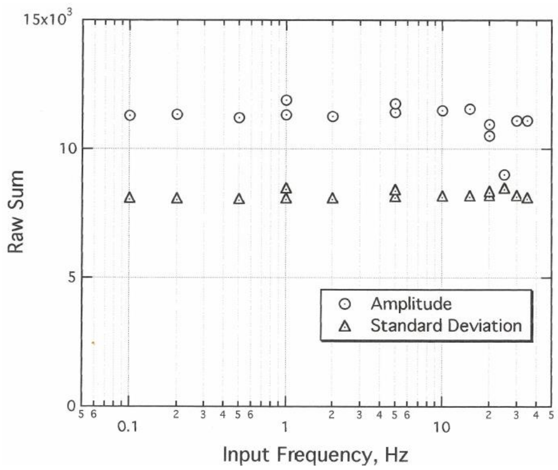

(a) Stepwise Loading (b) Sinusoidal Loading

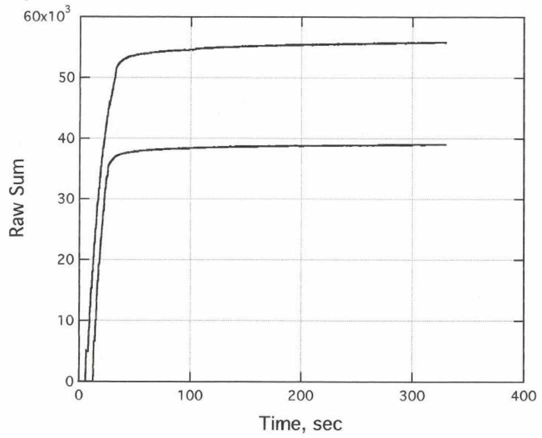

(c) Creep Test

Figure 1. Results of Trial Tests

MODEL TEST

Model Ships and Test Method

Two model ships were tested at NMRI ice tank. One is a 1:16 scaled model of an icebreaker (Shimoda et al., 2002) and the other is a 1:36 scaled model of an cargo ship (Izumiyama, 1995). Main dimensions of these models and ships are shown in Table 1. These model ships were designed for research projects and there are no actual existing ships for them. Both model ships have a conventional wedge-shaped bow with V-shaped frame lines. The icebreaker model is equipped with twin podded propulsors ( ), while the cargo ship model has a conventional propulsion system with a single propeller and a rudder.

Table 1. Main Dimensions of Models and Ships

(a) Icebreaker

	Model	Ship
Length, m	4.688	75.0
Width, m	0.857	14.0
Draft, m	0.250	4.0

(b) Cargo Ship

	Model	Ship
Length, m	4.861	175.0
Width, m	0.667	24.0
Draft, m	0.222	8.0

Eight tactile sensor films were installed on the model ship hulls along the water line from the bow to the stern. Figure 3 shows tactile sensor locations for the icebreaker model. Model ships were tested in in a free-running mode where they had six degrees of freedom in motion. Tests were performed in level ice with thickness of 0.50 m and 0.8 m for the icebreaker and 1.0 m for the cargo ship in full-scale. Turning tests as well as straight-going tests were performed. In some tests an S-shaped turning was made. Figure 4 shows an S-shaped turning track by the icebreaker model.

Figure 2. Podded Propulsors

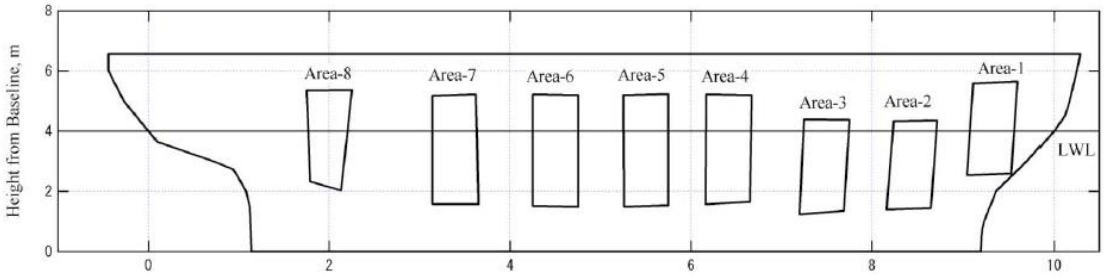

Figure 3. Tactile Sensor Areas on Icebreaker Model

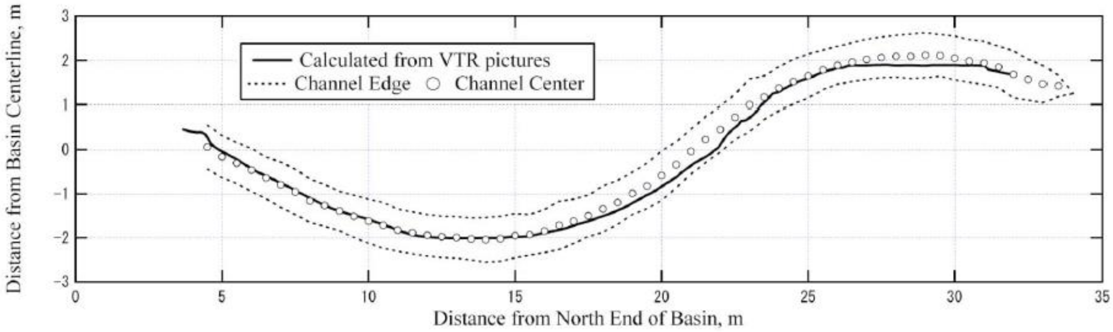

Figure 4. Model Ship Track in S-shaped Turning Test

Analysis

In a full-scale measurement, local ice loads on the hull are usually measured by strain gauges installed on transvers frames. Ice load on each frame is calculated from the strain measured. Analysis of the tactile sensor data was done so that it can be comparable with this full-scale measurement method. For this purpose the sensor was divided into 11 narrow vertical segments. Each segment is of 4 sensing cells in width and of full sensor height (Figure 5). The width of a segment is 0.35 m and 0.79 m in full-scale for the icebreaker and cargo ship, respectively. Ice load on each segment was calculated. The ice load value of non-exceedence probability of 99% was taken as the representative value for the local ice load on the segment.

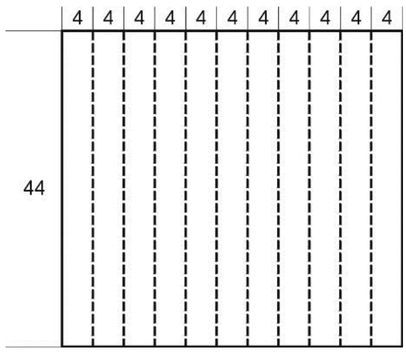

Figure 5. Data Analysis Segments

Results

The I-Scan system has a function to display measured pressure as a two-dimesional distribution map.

Figure 6 is an example of such display window. Loaded cells are colored. Data measured in the bow of a model ship is shown. Load patches of short length are aligned in a line forming a “broken-line-like” pattern. The load patch line moves sternward and downward as the model moves in ice.

Figure 7 (a) shows a time curve of local ice load acting on a data analysis segment. Ice load shows a spike-like pattern with many peaks. These peaks were recorded as a load patch passes over the data analysis segment. Figure 7 (b) shows a time curve of local ice load measured in a full-scale test performed in the Sea of Okhotsk. (Uto et al., 2005). Full-scale ice load also shows a spike-like pattern with many peaks as observed in the model test result.

This similarity indicates that full-scale ice load also acts on load patches of short length moving sternwards.

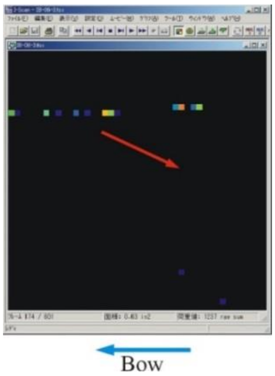

Figure 6. Ice Load Patch Pattern

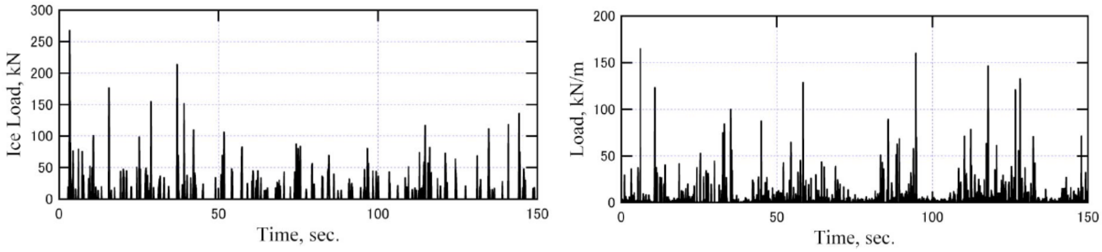

(a) Model Test Result (b) Full-Scale Data

Figure 7. Time Curves of Local Ice Load

Figure 8 shows ice load distribution along the hull in the straight-going tests for icebreaker and cargo ship. Ice load data measured by eight sensor films were plotted against the locations of the films on the model hull. These data are mean of representative values of ice load from 11 data analysis segments in a sensor film. Figure 9 shows ice load distribution in the turning tests. Ice load data in the inside of the turn are shown.

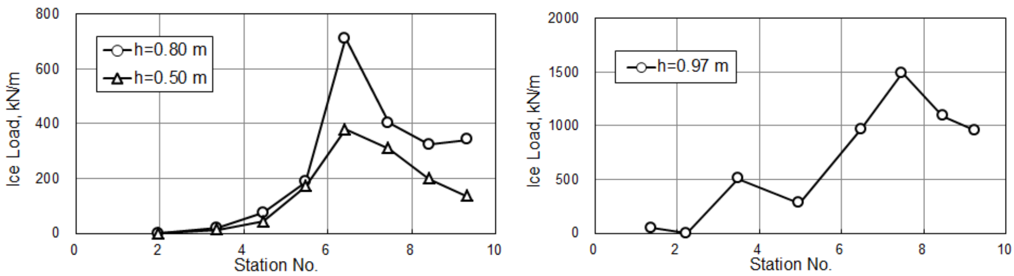

(a) Icebreaker (b) Cargo Ship

Figure 8 Ice Load Distribution in Straight-going Mode

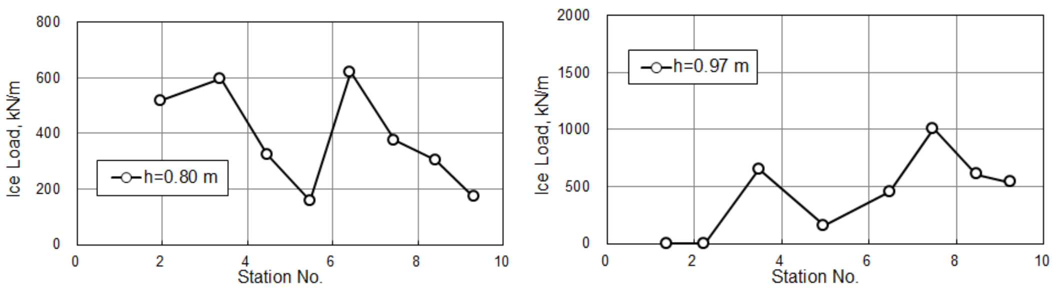

(a) Icebreaker (b) Cargo Ship

Figure 9. Ice Load Distribution in Turning Mode

DISCUSSION

Sensor Calibration

I-Scan sensor needs to be calibrated to obtain load value from digital counter Raw. However, calibrating the sensor for the purpose of ice model testing is not straightforward. Figure 10 shows the reason for this (Izumiyama et al., 1999a). The figure shows the result of a test in which loads are applied on individual sensing cells. Six cells were loaded over the entire cell area of 3.5 mm square (open circles). Outputs from these cells agree well each other indicating good spatial uniformity of the sensor film. Another cell was loaded only in a quarter of the cell area (full circles). Outputs from this cell significantly differ from those of entirely loaded cells for same loads. The test shows that the output from the I-Scan sensor system depends not only on the load applied but also on the area on which load acts, or more generally, contact conditions at the interface.

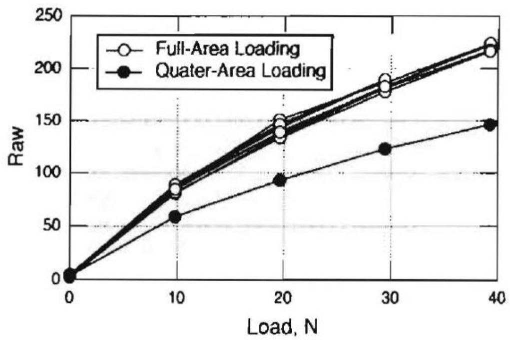

Figure 10. Loading on Individual Cells

However, it is difficult to know the actual contact conditions at the interface for solid-solid contact problems including hull-ice contact. Actual contact area may differ from the virtual one. Pressure cannot be uniform but vary within a contact area. In the case of hull-ice contact, local ice failure at the interface will make the problem more complicated. Based on this consideration, it was decided to calibrate the I-Scan system by using ice load acting on the model. In this way, the effects of the above-mentioned complexity related

to the hull-ice contact conditions can be included in the calibration.

In the present model test, resistance is used for the calibration of the I-Scan system (Matsuzawa et al., 2006). Resistance of the model is given as a vector sum of local ice loads on the model hull. Sensor films gives Raw Sum corresponding to local ice loads normal to the model surface. Longitudinal component of those Raw Sums are calculated using hull angles at the location of sensor films and summed up over the bow region of the model. Raw Sum for the hull areas between sensor films are interpreted from data of neighboring films. Calculated value was doubled to account for resistance on the other side of the model where sensor films are not installed. Resistance was calculated from propeller thrust assuming a thrust deduction factor. Figure 11 shows the correlation of Sum of longitudinal Raw Sums and resistance of the model. Dashed line in the figure was used for the sensor calibration in the present model test.

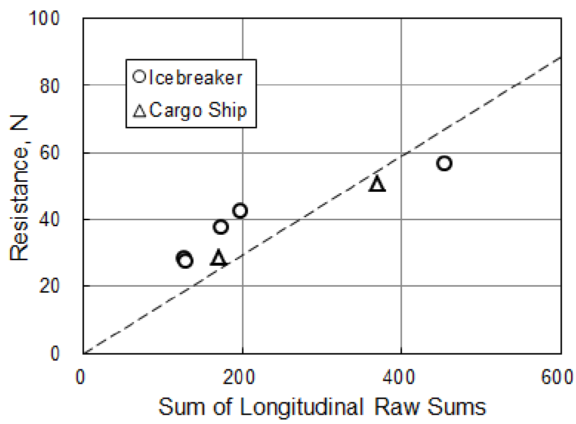

Figure 11. Calibration Line

Ice Load in Straight-going Mode

In the straight-going test, ice loading is predominant in the bow region as shown in Figure 8. This ice load distribution results from the way the bow breaks the ice (Figure 12). With a very few exceptions, ice-going ships are designed to break ice in bending by an inclined bow. When a ship sails in ice, the inclined bow pushes the ice downwards. Ice then breaks with a crack running some distance away from the contact point forming a broken ice piece. The ice piece is further pushed down to be submerged and a new contact takes place. The process is repeated to form an open channel in the ice. The bow is exerted by loads when it bends, breaks and submerges the ice. Hull-ice contacts and ice loading take place at many points on the bow. Ice loading in the ship region after the bow is much more moderate than that in the bow as the channel formed by the bow is wider than the ship beam and there is less chance for the hull to contact the ice.

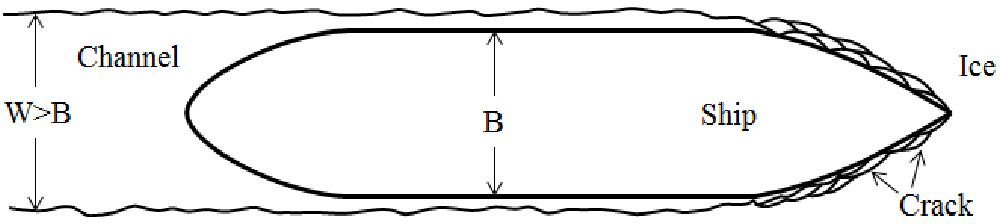

Figure 12 Schematic of Ship and Channel in Ice

Difference in ice load intensity in different hull regions is taken into account in the design ice loads calculation in ship design rules. Figure 13 shows a factor defined in Finnish-Swedish Ice Class Rules (FSICR), a *de facto* standard for ship design for first-year ice conditions, to calculate design ice loads. The factor "takes account of the probability that the design ice pressure occurs in a certain region of the hull for the ice class in question". The factor gives design ice loads for the midbody and stern regions relative to the bow (factors for the bow is always unity). FSICR defines four ice classes of IA Super, IA, IB and IC with IA Super being the highest and IC the lowest. Figure 13 shows factors for these ice classes. The factor decreases from the bow toward the stem. The lower the ice class is the more the factor is reduced for the midbody and the stern.

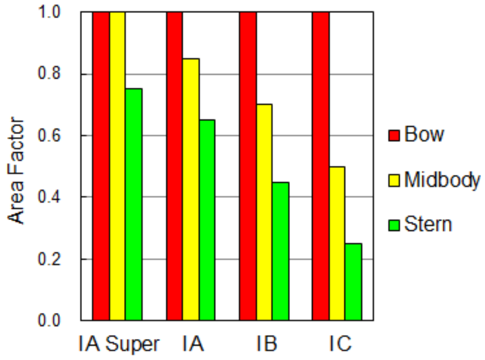

Figure 13. Factors defined in FSICR

In the bow region, the ice load increases from the stem toward the fore shoulder. It is interesting to see this ice load distribution in regard with hull angles of the bow. Varsta (1983) performed a numerical calculation of ice load acting on a ship bow. His calculation showed the ice load is a function of the inclination angle (angle off the vertical) of the hull as shown in Figure 14 (a). Ice load increases with the decrease of the angle. Result of the model test is shown in Figure 14 (b). In the figure, non-dimensional ice load (ice load divided by resistance) is plotted against the spread angle of the model hull. Model test result also shows that ice load increases with the decrease of the hull angle.

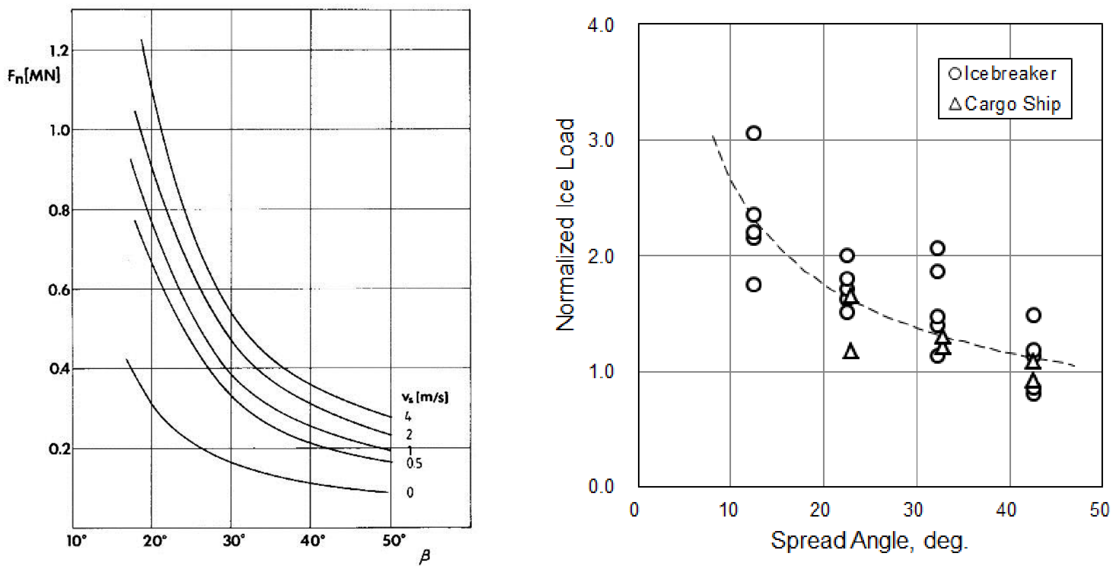

(a) Ice Load Calculation by Varsta (1983) (b) Model Test Result

Figure 14. Effects of Hull Angle on Ice Load

Ice Load in Turing Mode

In the turning mode, ice load distribution along the hull is totally different from that in the straight-going mode (Figure 9). The stern, not only the bow, is exerted by significant ice loading. This can also be explained by ship motion in the open channel (Figure 15). When a ship turns in ice, force from the rudder or propulsor pivots the ship in the channel. The aftbody of the ship is pressed against the edge of the channel and thereby exerted by loads from the ice.

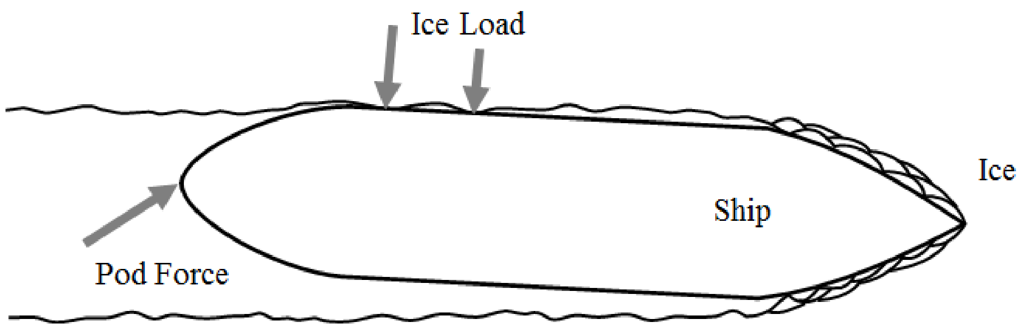

Figure 15. Schematic of Ship Pivoting in Channel

Ice loading in the stern is more notable for the icebreaker model with podded propulsors than the cargo ship model with the conventional rudder and properllar system. This is due to high lateral force from the propulsors to turn the model. Figure 16 shows correlation of ice load measured in sensor films located in the stern of the icebreaker model and lateral force of the pods. Stern ice load increases as the pod force increases.

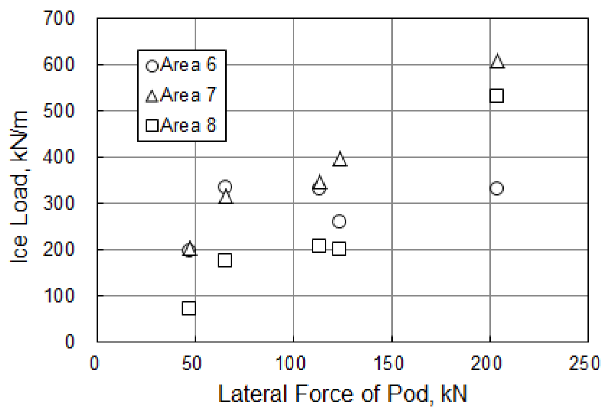

Figure 16. Correlation of Stern Ice Load and Lateral Force of Propulsors

Podded propulsors are increasing utilized in ice-going ships in recent years. Those ships show superb manoeuvrability in ice (e.g.: Nyman et al., 1999). Test results shown in Figure 16 indicate that such ships with podded propulsor could receive high ice loads in the aft region as well as the bow. It may not be relevant to use factors shown in Figure 13 to calculate design ice loads for those ships. Regarding this matter, FSICR states "The introduction of new propulsion arrangements with azimuthing thrusters or "podded" propellers, which provide an improved manoeuvrability, will result in increased ice loading of the Stern region and the stern area. This fact should be considered in the design of the aft/stern structures." However, no rule is given for how it should be "considered" in the ship design. This may be attributed to the lack of full-scale data from ships with podded propulsors. Accumulation of such data is needed.

Comparison with Full-scale Data

Model testing is performed so that the similarity law holds between the model- and full-scale conditions. For ship model testing in ice, the similarity law requires the followings.

$$l_S = \alpha l_M, \quad \sigma_S = \alpha \sigma_M, \quad t_S = \alpha^{1/2} l_M, \qquad (1)$$

where α is the scale ratio, l, σ and t are dimensions of ship and ice, ice strength and time, respectively. Suffices M and S refer to mode- and full-scale, respectively. For force, F , the cube law holds as

$$F_S = \alpha^3 F_M \, . \tag{2}$$

In the present analysis, full-scale local ice load was calculated from measured tactile data based on the above cube law.

As there are no real existing ships for the models tested, it is difficult to compare the ice load calculated from model test results with full-scale data directly. Instead, test results are compared with design ice loads calculated based on the ice load formula of FSICR. FSICR assumes ships of each ice class to operate in conditions corresponding to level ice thickness not exceeding the value shown in Table 2. Design ice load for the bow was calculated based on ice thickness of the model test and ice class corresponding to the thickness.

Table 2. Level Ice Thickness for FSICR Ice Classes

Ice Class	Ice Thickness
IA Super	1.0 m
IA	0.8 m
IB	0.6 m
IC	0.4 m

Figure 17 compares calculated ice load with design ice load. The figure shows frequency distribution of the ratio of measured and design ice loads. Although most of measured ice loads are lower than the design ice load, there are a few data higher than it. Design loads are loads expected to occur during a long return period, whereas the length of each run is only about 30 m that is 0.5 to 1 km in full-scale. If one takes this into account, it may be interpreted form the result shown in Figure 17 that the model test tends to overestimate the local ice loads on ship hulls.

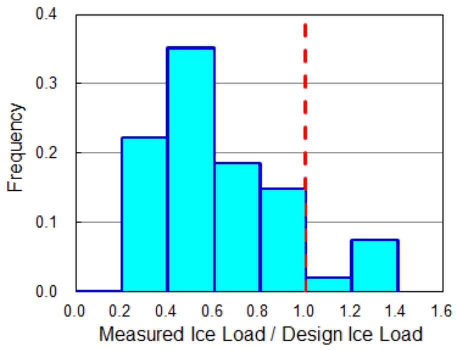

Figure 17. Comparison of Measured Ice Load and Design Ice Load

Local ice load occurs as a reaction force against the downward force to break ice in bending. Tactile measurement in the model test showed that hull-ice contact is “broken-line-like” consisting of short load patches (

Figure 6). Similarity between model- and full-scale load time curves (Figure 7) indicates that full-scale load patch is also broken-line like. It is reasonable to assume that the local ice load occur in individual load patch depends not only on the total load required to break ice but also on the contact condition between hull and ice. Figure 18 schematically shows ice loading in different contact conditions. Large local ice loads occur in a contact points (left), while the load is low when there are many contact points (right).

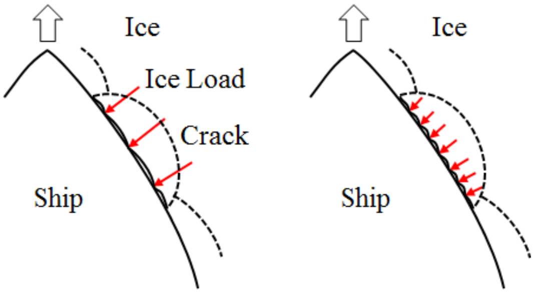

Figure 18. Schematics of Hull-Ice Contact and Local Ice Loads

Model ice has been developed mainly for the purpose of ship model testing. Mechanical properties of model ice are adjusted based on the similarity law so that it can properly simulate icebreaking by a ship including the downward force required to break the ice in bending and the way ice breaks. However, no study has been made of local contact conditions between ship hull and ice as discussed above to examine how model ice can be compared with sea ice in this regard. More study is required of this issue for ice model testing with tactile measurement to be a tool for estimating full-scale local ice loads as it is so for ship performance in ice.

There are two types of model ice in terms of the crystal structure – columnar and granular. Difference in model ice structure may lead to different contact conditions with models. The present test was performed in model ice with a columnar structure. Test in granular-structured model ice may give different results in regard with full-scale ice load estimation.

SUMMARY

This paper discussed local ice load measurement in model testing. A tactile sensor system is used for the model test at NMRI ice tank. Prior to the use for model test, the sensor system was tested by three different ways of loading to obtain basic characteristics of the sensor. Results of model test at NMRI ice tank were presented. Two model ships, one with podded propulsors and the other with conventional propeller and rudder system, were tested in a free-running mode. Discussion was made of the calibration of the tactile sensor, ice load distributions, and comparison of the test results with full-scale data. Output of the tactile sensor depends on contact conditions at the interface as well as load applied on it. Calibration of the tactile sensor needs considerations on this point. Local ice load is predominant in the bow when a ship is sailing straight. Stern is exerted by significant ice loading when a ship turns. Stern ice load correlates well with the lateral force of pods. Full-scale ice load is calculated based on the cube law. Calculated ice load is compared with design ice load. More study is required of local contact conditions between ship hull and ice to examine how model ice can be compared with sea ice in this regard.

REFERENCES

Hanninen, S., 2007. Inventory of Data Sources Available on Ship Hull Ice Loads and Damages. In: *Increasing the Safety of Icebound Shipping Final Scientific Report: Volume 1*, Helsinki University of Technology Ship Laboratory M-302, pp.22-33.

Izumiyama, K. and Uto, S., 1995. Ice Resistance of Three Bow Forms for the NSR Cargo Ship. Northern Sea Route; Future & Prospective, *The Proceedings of INSROP Symposium Tokyo '95 (1-6 October 1995)*, pp. 459-467.

Izumiyama, K., Wako, D. and Uto, S., 1999a. Ice Force Distribution on a Flat Indentor. In: Ice in Surface Waters, Shen (ed.), Vol. 2, pp. 917-922.

Izumiyama, K., Wako, D. and Uto, S., 1999b. Ice Force Distribuion around a Ship Hull. *Proceedings of the 15th International Conference on Port and Ocean Engineering under Arctic Conditions*, Vol. 2, pp. 707-716.

Izumiyama, K., Wako, D. and Uto, S., 2001. Ice Pressure acting over a Model Ship Hull. *Proceedings of the 16th International Conference on Port and Ocean Engineering under Arctic Conditions*, Vol. 2, pp. 793-802.

Izumiyama, K., 2007. Description of Local Ice Loading and Hull Area Factor on Model Test Results. In: *Increasing the Safety of Icebound Shipping Final Scientific Report: Volume 1*, Helsinki University of Technology Ship Laboratory M-302, pp.115-134.

Izumiyama, K., Uto, S., Otsubo, K., Matsuzawa, T., Shimoda, H., Wako, D., Asanuma, T. and Yamamoto, J., 2016. Ice Load Distribution on a Model Ship Station-keeping in Broken Ice. *Proceedings of the 31st International Symposium on Okhotsk Sea & Sea Ice*, pp. 92-95.

Jeong, S., Choi, K., Ha, J., Kang, K. and Cheon E., 2015. Distribution of Ice Load acting on Model Hull due to Ship-Ice Interaction. *Proceedings of the 23rd International Conference on Port and Ocean Engineering under Arctic Conditions*.

Kayo, Y., 1993. Measurement of Ice Load Distribution on an Icebreaker Bow Model composed by Loade Panels. *Proceedings of the 12th International Conference on Port and Ocean Engineering under Arctic Conditions*, Vol. 1, pp. 328-337.

Kujala, P. and Arughadhoss, S.., 2012. Statistical Analysis of Ice Crushing Pressure on a Ship's Hull dring Hull-Ice Interaction. *Cold Regions Science and Technology*, Volume 70, January 2012, pp. 1-11.

Liukkonen, S. and Nortala-Hoikkanen, A., 1992. Ice Resistance Tests on a Segmented Icebreaker Model. *Proceedings of the 11th IAHR International Symposium on Ice*, Vol. 1, pp. 296-308.

Matsuzawa, T., Wako, D. and Izumiyama, K., 2006. Local Ice Load on a Ship with Podded Propulsors. *Proceedings of the 18th IAHR International Symposium on Ice (2006)*, Vol. 2, pp. 33-40.

Nyman, T., Riska, K., Soininen, H., Lensu, M., Jalonene, R., Lohi, P. and Hrjula, A., 1999. The Ice Capability of the Multipurpose Icebreaker Bothnica – Full Scale Results. *Proceeding of the 15th International Conference on Port and Ocean Engineering under Arctic Conditions*, Vol. 2, pp. 631-643.

Shimoda, H., Wako, D., Takimoto, T., Tamura, K. and Uto, S., 2002. Development of an Icebreaking Patrol Vessel with Podded Propulsors – Basic Design and Open Water Performance – (in Japanese). *Proceedings of 2002 Cold Region Technology Conference*, pp. 204-210.

Transport Safety Agency of Finland, 2010. Finnish-Swedish Ice Class Rules 2010. p. 48.

Valkonen, J. Izumiyama, K. and Kujala, P., 2007. Measuring of Ice induced Pressures and Loads on Ships in Model Scale. *Proceedings of the 10th International Symposium on Practical Design of Ships and other Floating Structures*.

Uto, S., Murakami, C., Takimoto, T. and Izumiyama, K., 2005. Ice Load exerted on the Hull of Icebreaker PM Teshio in the Southern Sea of Okhotsk. *Proceeding of the 18th International Conference on Port and Ocean Engineering under Arctic Conditions*, Vol. 2, pp. 683-692.

Varsta, P., 1983. On the Mechanics of Ice Load on Ships in Level Ice in the Baltic Sea. *Technical Research Center of Finland, Publication 11*, p. 91.